

# Chapter 9

## Imaging Modalities

Kenneth H. Wong

### Abstract

This chapter provides an overview of the different imaging modalities used for image-guided interventions, including x-ray computed tomography (CT) and fluoroscopy, nuclear medicine, magnetic resonance imaging (MRI), and ultrasound. The emphasis is on the distinguishing physical and engineering properties of each modality and how these characteristics translate into strengths and weaknesses for the end user. Because the imaging methods are very different, there is no single ideal modality for image-guided interventions; rather, they are largely complementary and can all provide valuable information about the patient. The chapter also covers current research topics in medical imaging relating to image-guided interventions and how these trends could potentially improve image-guided interventions in the future.

### 9.1 Introduction

A wide array of medical imaging modalities is in use currently, and almost all of them have been integrated into some form of image-guidance system. An exhaustive treatment of these different modalities is far beyond the scope of this chapter, but many excellent reference textbooks are available [Bushberg et al. 2002; McRobbie et al. 2003; Webb 2002]. The goal of this chapter is to provide an introductory level overview and comparison of these modalities in the context of image-guided intervention systems, addressing the perspective of both the system designer and the practitioner. Some knowledge of basic physics, engineering, and anatomy is assumed. The information in this chapter should help the reader to:

1. understand basic physical and engineering principles of each imaging modality, including key limitations, such as spatial resolution, temporal resolution, and field of view;

2. understand the types of biological and physiologic information that can be obtained from the different modalities; and
3. compare the advantages and disadvantages of different imaging modalities for image-guided intervention applications.

The following modalities are covered in this chapter: x-ray fluoroscopy, x-ray computed tomography (CT), nuclear medicine, magnetic resonance imaging (MRI), and ultrasound. These five are the most commonly used modalities for image-guided interventions.

## 9.2 X-Ray Fluoroscopy and CT

### 9.2.1 Basic Physics Concepts

Both fluoroscopy and CT utilize x-rays to form images and so there are some common features that will help us to understand the performance of these systems. X-rays are generated by accelerating electrons and directing them toward a metal target, as shown in Fig. 9.1.

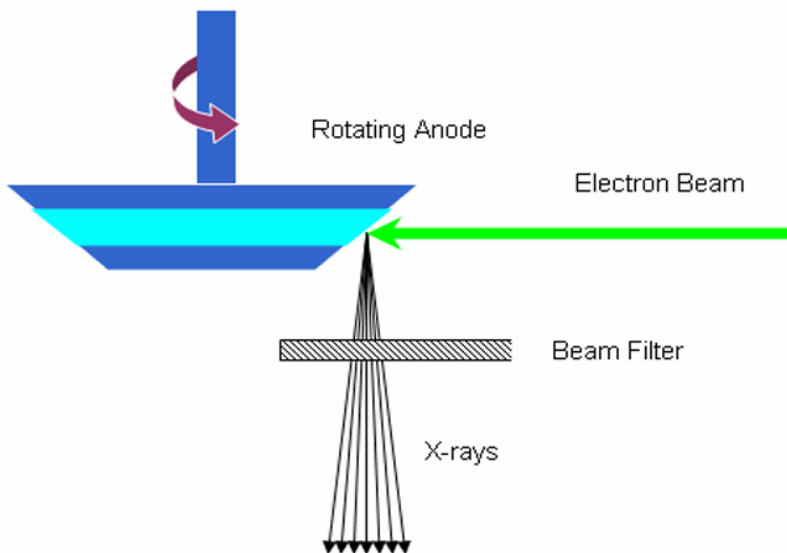


**Fig. 9.1.** Schematic of a simple x-ray generator. The electron beam impacts the anode and creates x-rays via bremsstrahlung (braking radiation). The anode rotates to dissipate heat from the electron beam, and in many cases is also liquid cooled. A filter removes low-energy x-rays from the beam, since these would only be absorbed in the patient and would not contribute to the formation of the image

The electrons rapidly decelerate upon encountering this material, dissipating their energy as heat and bremsstrahlung (braking radiation) x-rays. The electron source is focused so that the x-rays are emitted from what is essentially a small point source, resulting in a divergent cone beam of x-rays.

Typical x-ray generators have a maximum electron acceleration voltage between 70 and 300 kV, so the maximum energy of the emitted x-rays ranges from 70 to 300 keV. However, the peak of the resulting x-ray spectrum is at approximately one third of the maximum energy. Furthermore, thin metal transmission filters remove lower energy x-rays from the spectrum, so the final spectrum reaching the patient is similar to the one shown in Fig. 9.2.

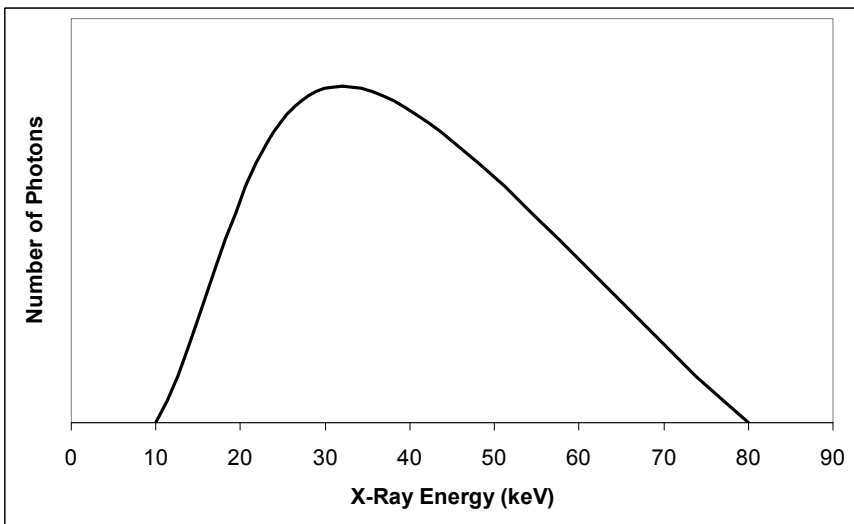


**Fig. 9.2.** Simulated x-ray spectrum. The bremsstrahlung process produces x-rays of all possible energies up to the maximum energy of the electron beam, but low-energy x-rays are removed from the beam by self-filtering in the anode and external beam filters. Depending on the application, the beam filters can be changed to allow more or less of the low-energy photons to reach the patient

The x-ray photons travel in straight lines from the source. Given the typical x-ray energies involved in fluoroscopy and CT, the x-ray photons interact with the patient through the photoelectric effect and Compton scattering. These mechanisms are dependent on the x-ray energy, elemental composition of the tissue, and tissue density. In the human body, this means that structures with a higher content of calcium and phosphorous (such as bones) will be more attenuating than soft tissues. Similarly, tissues with low density (such as the lungs) will be less attenuating than fat or muscle.

Photons interacting through the photoelectric effect are essentially absorbed in the patient and do not reach the detector. Compton scattered photons may be scattered in any direction, so a significant number of these photons could potentially reach the detector. However, since the location of the scattering cannot be determined, these scattered photons do not carry any useful imaging information. Thus, a grid of small metal vanes is placed in front of the detector so that the scattered photons will be absorbed in the grid rather than detected.

The net result of this imaging approach is that the detected x-rays are considered to have traveled in a straight line from the source to the detector, and the number of photons reaching the detector (typically expressed as  $I/I_0$ , where  $I$  is the intensity at the detector and  $I_0$  is the initial beam intensity) is based on the density and elemental composition of the tissue along that line. X-ray images are often described as shadowgrams or projection images.

Since both fluoroscopy and CT use x-rays for image formation, image-guided procedures using these modalities expose the patient, physician, nurses, technologists, and other staff to potentially hazardous radiation. When considering risk from x-ray exposure during a procedure, it is important to remember that the medical personnel using the equipment are most affected, since they work with the equipment on a daily basis, whereas patients usually are exposed only during a few visits. To mitigate these risks, x-ray imaging systems have several common safeguards. First, many x-ray sources are designed with feedback systems that regulate the tube output. These systems try to maintain a constant flux on the detector, and will lower the tube output in areas of the body, such as the lungs, where organs are less dense. This approach minimizes the dose while maintaining a constant level of image quality. Second, manually operated sources, such as those in fluoroscopy, have dose counters and timers to prevent inadvertent overexposure. Third, advances in detector sensitivity have enabled significant dose reduction, and this trend is likely to continue. Finally, professional and regulatory agencies such as the International Commission on Radiation Protection (ICRP) and the Food and Drug Administration (FDA) have promulgated guidelines for fluoroscopy training and credentialing, which help to ensure proper training and awareness of risks related to x-ray image guidance [Valentin 2000; Archer 2006].

## **9.2.2 Fluoroscopy**

### **9.2.2.1 System Components**

An example of a fluoroscopy system is shown in Fig. 9.3. The x-ray generator and the detector are mounted facing each other on a curved arm (commonly referred to as a C-arm). The patient table lies between the



**Fig. 9.3.** Fluoroscopy system. The patient table is shown in the foreground, and viewing monitors for the fluoroscopy images are visible in the upper right of the photo. One C-arm is mounted on a rotating floor plate that allows it to move in and out from the patient table, and the other is mounted on rails in the ceiling that allow it to move around the room. The C-arm closest to the table is oriented so that the x-ray generator is below the table and the image intensifier is above the table

generator and the detector, and the arm can be rotated around the patient so that the fluoroscope image can be acquired from any angle.

The traditional fluoroscopy detector is an image intensifier that uses a scintillator to convert the x-rays into visible light. The visible light is then converted to an electronic signal, amplified, and then converted back into a video image that can be displayed on a monitor and/or recorded on video tape. Recently, digital detectors have been developed to replace the image intensifier. In addition to being more compact, the digital detectors have far less image distortion and greater dynamic range, so it is likely that digital detectors will eventually supplant the image intensifier, much as flat-panel monitors have replaced cathode ray tubes (CRTs) in personal computers.

### 9.2.2.2 Image Characteristics

An example of a fluoroscopy image is shown in Fig. 9.4. The spatial resolution of fluoroscopy is high so that submillimeter-sized objects can be resolved. This 2D image clearly shows the contrast between different materials (such as bone and liver) and different tissue densities (such as the heart

and lungs). However, this does not apply to soft tissue structures, such as the heart chambers or the lung airways, which cannot be resolved. The image also reveals a key limitation of 2D imaging, which is that overlying structures are all reduced to a single imaging plane. This overlap is an unavoidable consequence of projection imaging.

One advantage of a pure projection imaging technique is that no post-processing or reconstruction is required, so fluoroscopy is a real-time,

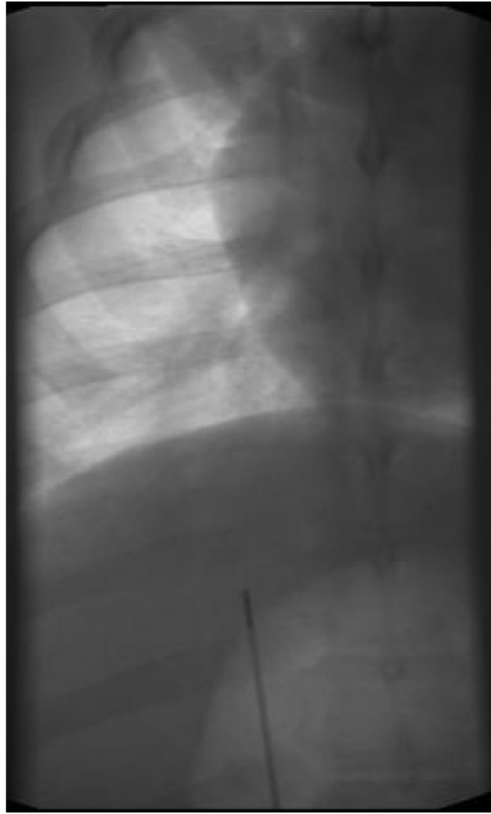


**Fig. 9.4.** Fluoroscopy image of a swine chest. The ribs, heart, lungs, and diaphragm are clearly visible because of their large variance in contrast. A metal needle implanted into the liver is also easy to see. However, internal soft tissue structures such as vessels in the liver or airways in the lungs cannot be seen. The projection image covers a large region of the body, but does not provide any depth information; for example, the barrel shape of the ribcage is flattened into a single plane

imaging method.<sup>1</sup> Fluoroscopy users can immediately observe changes in the patient or the transit of tools and catheters inserted into the patient. For these reasons, fluoroscopy is used extensively in interventional radiology, cardiology, and electrophysiology, and is seeing increasing use for image-guided oncology therapies such as radiofrequency ablation (RFA).

### **9.2.2.3 Patient Access and Work Environment**

Fluoroscopy is the workhorse modality for interventional radiology, and thus systems for fluoroscopy are designed with patient access as a primary goal. The x-ray generator and the detector are relatively small and do not create much of an obstruction for the physician. The C-arm gantry also can be rotated to move the components somewhere more unobtrusive. Furthermore, both the C-arm gantry and the patient table can be translated apart from each other or close together to modify the workspace for the physician. Some C-arm systems are even designed to be portable, so that they can be easily moved in and out of operating rooms or other locations in the hospital where x-ray imaging is needed.

## **9.2.3 Computed Tomography**

### **9.2.3.1 System Components**

In CT, the x-ray generator and detector are mounted on a gantry that rotates around the patient as he or she lies on a movable bed. An example photograph of a CT scanner is shown in Fig. 9.5.

The majority of current CT systems are based on fan-beam geometry, where the x-ray beam is collimated to match an arc-shaped detector on the opposite side of the gantry. The minimal configuration of detectors in this geometry is a single row, but as detector design and electronics speed have improved, multiple rows of detectors or large detector panels are used, as illustrated in Fig. 9.6. By increasing the detector area, the system can image a larger area of the body in a single exposure, which allows for faster scanning. Modern multidetector CT systems can acquire an entire image of the torso in just a few seconds.

---

<sup>1</sup> There are different definitions of “real-time,” but in this chapter we will define the term from an imaging perspective, where real time means that images are obtained at video rates (30 Hz) so that there is no perception of individual image frames.



**Fig. 9.5.** Photograph of a CT scanner used for image-guided interventions. This scanner has a CT fluoroscopy mode for acquiring images in near real time (approximately 6 frames/s), which enables CT-guided interventions

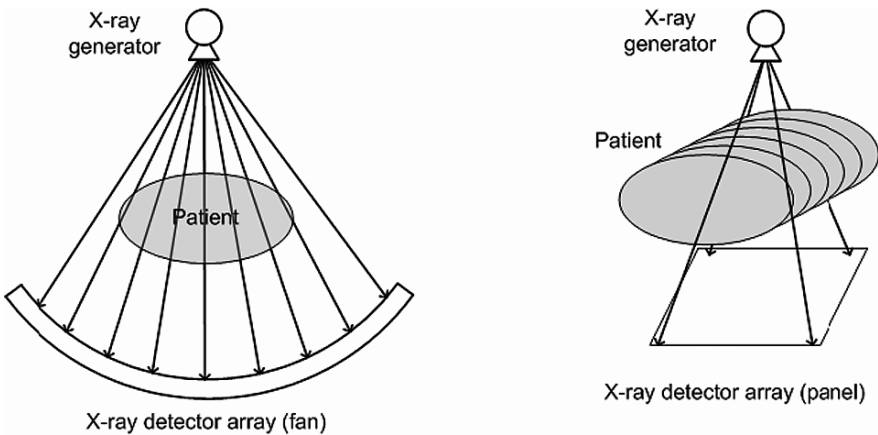


**Fig. 9.6.** CT system schematics showing fan beam geometry (*left*) and cone-beam geometry (*right*)

The detector usually is made from a solid scintillator or high-pressure xenon gas and is pixellated (typically on the order of 700–1000 elements), so the x-ray fan beam can be spatially sampled by individual elements, each having submillimeter width. When x-rays are absorbed in a detector element, the detector generates an electrical current that is then read by an



amplifier to form the detector signal. Because the source and the detector are in constant motion and it is necessary to acquire a number of angular samples comparable to the number of detectors, x-ray detectors in CT scanners operate at much higher sampling rates (several kilohertz) than those in fluoroscopy systems.

As the gantry rotates, projection images of the patient are acquired at fixed angular intervals. Once a sufficient number of angular samples have been obtained, the projection images are then mathematically reconstructed into 3D axial slices through the patient. Although the reconstruction process requires a fast or parallelized computer, x-ray CT reconstruction can be performed analytically using backprojection methods [Herman and Liu 1977; Lakshminarayanan 1975; Scudder 1978], and thus can be performed in almost real time.

### 9.2.3.2 Image Characteristics

Due to the excellent image quality of CT images, they are used extensively for pretreatment imaging and treatment planning, as discussed in Chapter 3: Visualization in Image-Guided Interventions. Using CT for direct guidance has some benefits over fluoroscopy, due to the ability to see structures in



**Fig. 9.7.** This CT image is an axial slice through the patient's pelvis. As with the fluoroscopy image, bones and air spaces are readily visible against the soft tissue background. The soft tissue, especially the boundaries, can be visualized more clearly than with fluoroscopy because overlapping structures are not compressed into a single plane

three dimensions, but the real-time performance is not as high as with fluoroscopy. To acquire sufficient projections for a CT image, the x-ray generator and detector must rotate at least  $180^\circ$  around the patient. The rotation speed of the gantry is limited to roughly 0.4 s per revolution for physical reasons, which corresponds to about 2 images per s, assuming an instantaneous reconstruction. Figure 9.7 shows an example of a CT image.

### **9.2.3.3 Patient Access and Work Environment**

The CT scanner environment offers less work area than fluoroscopy because of the large gantry. Although the patient bed can be translated in and out of the scanner for positioning and setup, the field of view of the CT scanner is limited to the portion of the patient that is inside the gantry. Accordingly, physicians must typically stand beside the gantry and lean over the patient, or extend their hands into the imaging region if the CT is used for direct guidance. An alternative strategy is to use an “advance and check” approach, where the interventional tool is moved a small distance with the scanner off, and then the patient is imaged again to determine magnitude and direction of the next move. In the hands of an experienced operator this iterative process can be very effective at minimizing patient dose and localizing a target, but such expertise is uncommon.

One limitation to the CT imaging approach is that the natural image plane of the CT system is axial, with the image plane running from left to right and anterior to posterior. This means it is difficult to track an object such as a catheter that is moving in a superior–inferior direction, because the object is only within the field of view of the scanner for a short time. For this reason, CT is used more for percutaneous procedures where the movement of the interventional tool is mostly within the axial plane, as opposed to intravascular procedures where the major vessels run perpendicular to the axial plane.

### **9.2.4 Current Research and Development Areas**

Given the different capabilities of CT and fluoroscopy, it is only natural that efforts are being made to combine the systems and provide dual-use capability for image-guided interventions. A handful of CT scanners now offer a CT-fluoroscopy mode where images can be generated at 4–6 frames per s. To accomplish this speed, the systems generate a reconstructed image from a full rotation, and then update that image using projection data from a partial gantry rotation. With this scheme, even if the gantry only rotates twice per second, new images can be generated at higher rates and still provide salient information, such as the location of an interventional probe.

The reverse approach is to provide CT-like capabilities in the fluoroscopy environment. Since the x-ray source and detector of a fluoroscopy system are already mounted on an arm that can rotate around the patient, it

is possible to acquire multiple projections with the fluoroscopy system and use these projections to reconstruct a 3D image of the patient. In this approach, the detector is an area detector, and the x-ray beam is collimated into a cone rather than a fan (as shown on the right side of Fig. 9.6), and so the technique is generically referred to as cone-beam CT (CBCT).

Although this concept has always been theoretically possible with fluoroscopy systems, limitations of the image intensifiers used in fluoroscopy prevented it from being used on a widespread basis, although prototype systems were successfully demonstrated [Endo et al. 1998]. With the advent of fully digital x-ray detectors and improved mechanical control of the fluoroscopy system, tomographic imaging options for fluoroscopy are now being offered by all major medical imaging equipment vendors. Similar systems are also being used in radiation medicine applications to provide setup and or intra-treatment imaging [Jaffray et al. 2002].

## 9.3 Nuclear Medicine

### 9.3.1 Basic Physics Concepts

Nuclear medicine encompasses two different imaging techniques: positron emission tomography (PET) and single photon emission tomography (SPET), which is also commonly referred to as single photon emission computed tomography (SPECT). In nuclear medicine, the patient is injected with a radioactive tracer that has some useful biochemical properties. For example, the tracer may distribute in proportion to glucose metabolism, or bind to a particular molecule preferentially expressed on cancer cells. Upon decay of the radioactive atom attached to the tracer, either a positron or gamma ray is emitted. In the case where a positron is emitted, the positron quickly encounters an electron in the body and the two annihilate each other, creating a pair of gamma rays.

The gamma rays are high-energy photons and are considered to move in straight lines from the source. As with x-ray imaging, the gamma rays are attenuated by the photoelectric effect and Compton scattering. However, the detectors used in nuclear medicine have important differences from those in x-ray imaging. First, unlike in x-ray systems, the precise source location is not known in advance, but the photon energy is known because the emissions from radioactive nuclei are monoenergetic. A nuclear medicine detector rejects scattered radiation by determining the energy of each detected photon; if the original photon scatters in the body before reaching the detector, its energy will have been reduced by the scattering event. Second, because the source location is not known in advance, the nuclear medicine detector must have some other way of determining where the photon originated. The means of accomplishing this is different for PET and SPET, and will be discussed in more detail in the following sections.

Finally, the number of photons used to form a nuclear medicine image is typically orders of magnitude lesser than the number required to form an x-ray image. The detectors in nuclear medicine are therefore specifically designed to operate at these much lower event rates. This low event rate also means that nuclear medicine images require a longer time to acquire (tens of minutes) and also contain more noise.

### 9.3.2 Positron Emission Tomography

#### 9.3.2.1 System Components

A system for PET is illustrated in Figs. 9.8 and 9.9.



**Fig. 9.8.** Photograph of a combined CT/PET scanner. Nearly all PET scanners sold today are this type of combined unit. The scanners are arranged in tandem inside a single housing, so that the patient bed can easily move the patient from one scanner to the other. In this case, the CT scanner is on the proximal end of the gantry, and the PET scanner is on the distal end of the gantry

When the positron and the electron annihilate, the gamma rays are emitted in opposite directions. The typical PET detector setup is therefore a ring or cylinder of detectors around the patient, so that both of these photons can be detected. Since both emitted photons have the same speed, they will

both reach the detector at almost exactly the same time.<sup>2</sup> If the PET system detects two photons within a short time window, these photons must have come from the same position, and that position lies somewhere along the line connecting the two detectors.

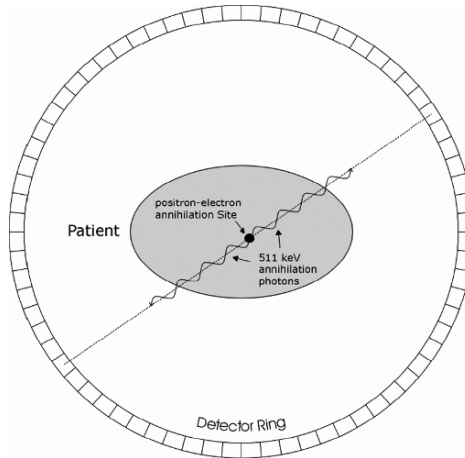


**Fig. 9.9.** Schematic for a PET scanner. The patient is surrounded by a ring or cylinder of detectors so that photons emitted in all directions can be captured

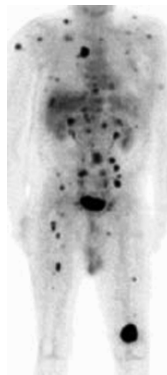


**Fig. 9.10.** Example of a PET image. This is a coronal view covering a region from the neck to the lower legs. Darker regions correspond to areas of increased radiotracer concentration, and therefore regions of suspected cancer involvement

<sup>2</sup> The gamma ray photons travel at the speed of light, so if the photons were emitted from the exact center of a typical PET system, they would reach the detectors approximately 1 ns later. If the photons were emitted close to the edge of the patient, there would be roughly a 0.5 ns difference between the detection times of the two photons. As long as two photons are detected within a few nanoseconds of each other, they are considered to have come from the same positron decay.

### 9.3.2.2 Image Characteristics

An example PET image is shown in Fig. 9.10. Although some anatomical structures can be discerned, the more salient features of the image are the numerous dark spots throughout the body, which correspond to metastatic cancer in those locations.

## 9.3.3 Single Photon Emission Tomography

### 9.3.3.1 System Components

A SPET system is illustrated in Figs. 9.11 and 9.12. SPET cameras localize the emissions coming from the patient by using a collimator, which contains thousands of thin channels that only admit radiation on a path perpendicular to the detector face. Photons reaching the detector are converted to visible light by a large scintillator crystal. This crystal is read out by an array of photomultiplier tubes, which determine the location where the photon entered the crystal by finding the centroid of the light recorded in all of the photomultipliers.

### 9.3.3.2 Image Characteristic

An example of a SPET image is shown in Fig. 9.13. As with the PET image, the image is more blurry and noisy than a CT image, and identification of structures is more difficult. Spatial resolution in SPET images is slightly worse than those of PET images, because the collimator imposes a distance-dependent blurring on the reconstructed image. Typical SPET systems have a resolution in the order of 6–9 mm.

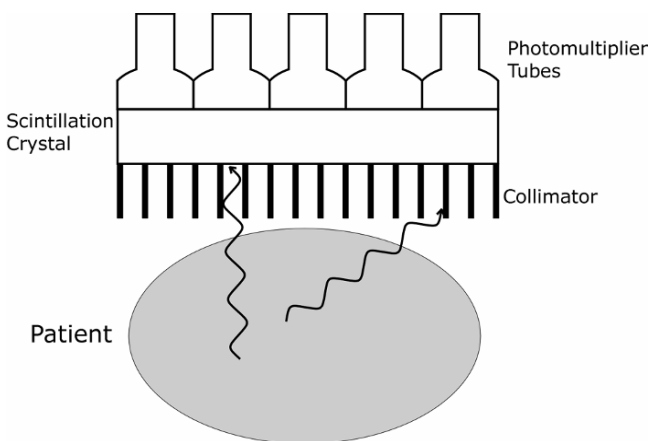


**Fig. 9.11.** Schematic of a single-head SPET scanner



**Fig. 9.12.** Photograph of a SPET scanner. This SPET scanner shown in the photograph has two imaging cameras, one above the patient bed and one below the patient. The cameras are mounted on a gantry that allows them to rotate around the patient in order to collect projection data from multiple angles

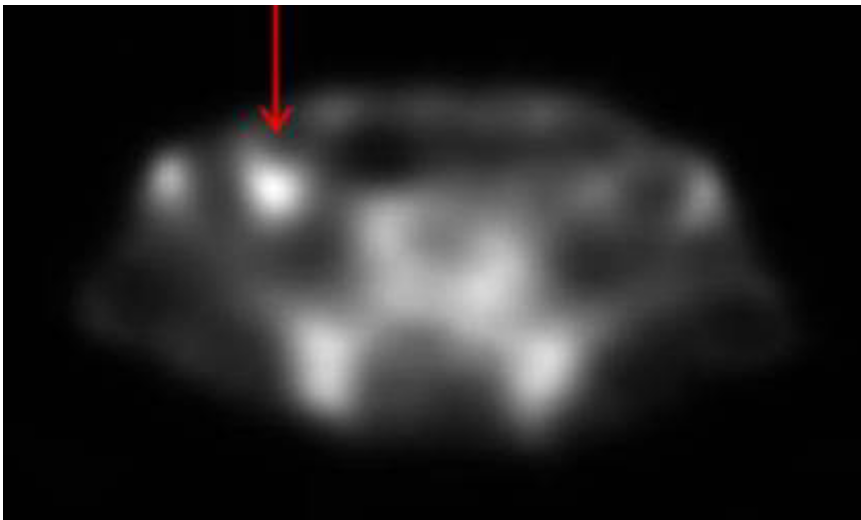


**Fig. 9.13.** Example SPET image of the pelvis (axial orientation). This patient has been injected with a radiotracer that binds to prostate cancer cells. Bright areas in the image correspond to areas of increased radioactivity concentration. The arrow on the top of the image indicates a potential area of disease, although other areas of the image are equally bright, reflecting nonspecific uptake of the tracer in the digestive and skeletal systems

### **9.3.4 Patient Access and Work Environment**

Both PET and SPET are designed as diagnostic imaging systems and are rarely used for direct image guidance. As with a CT system, the patient can be moved in and out of the gantry by translating the patient table, and for SPET the detectors can be rotated around the patient, so that access to the patient is similar to that available in a CT system. However, the major limitation for using PET and SPET for image guidance is that neither of them is a real-time imaging modality. Because the number of photons being emitted from the patient per second is significantly lower than the number of photons used to form an x-ray image, it is necessary to image the patient for longer periods of time. Even in the last decade, scan times in excess of an hour were not uncommon for whole-body imaging. Although the acquisition times have been much reduced by advancements in scanner technology and are currently on the order of a few to tens of minutes, the images still cannot be obtained in real time. Furthermore, PET and SPET reconstruction must be done using iterative methods that require significantly more computation time or power than the reconstruction methods used in x-ray CT, which further limits the speed at which images can be acquired and displayed to a physician.

Because radioactive materials are used in PET and SPET, these procedures carry some of the same risks that occur with x-ray imaging. However, because the number of photons used to form an x-ray image is much larger than the number of photons used to form a nuclear medicine image, the risk of overdose, acute radiation injuries, or long-term side effects is much lower in nuclear medicine than in x-ray imaging.

### **9.3.5 Current Research and Development Areas**

PET and SPET provide unique biological information about the patient, and could potentially be ideal for oncologic interventions where a critical question is to determine whether or not a particular region of the body contains cancer cells. As such, there are numerous emerging research efforts designed to overcome the limitations of nuclear medicine imaging and to make it more compatible with image-guided interventions.

One approach is to combine the biochemical imaging data from PET/SPET with an anatomical imaging modality such as CT or MRI. In this scheme, the anatomical image provides a structural road map of the body, and the nuclear medicine image provides the functional status of locations within the anatomy. The fusion of these two types of modalities has been widely accepted in diagnostic imaging since the first systems were proposed for CT/SPECT [Hasegawa et al. 1990] and CT/PET [Beyer et al. 2000], and in the current medical imaging marketplace the stand-alone full-body PET scanner has been wholly replaced with combined PET/CT systems.



Since, for example, a CT image can be obtained much more quickly than nuclear medicine images, the nuclear medicine data can be registered in advance to a planning CT image. These registered data sets can then be used for image guidance by registering the planning CT to a CT or fluoroscopy data set acquired during an intervention. Once one has obtained the mapping between the planning CT and the current x-ray image of the patient, it is then possible to use a similar function to map the preregistered nuclear medicine data into the current x-ray image.

An alternative approach is to redesign the nuclear medicine detection systems for real-time use. In most cases, this involves replacing the large nuclear medicine camera or gantry with compact detectors. In some cases, these detectors are no longer imaging systems, but instead are directional probes that provide an audio feedback based on the rate of detected photons. Although these devices do not provide true image guidance, they provide information about the patient which could not be obtained through other means and thus have found an important niche role in certain procedures, such as sentinel lymph node biopsy for breast cancer [Gulec et al. 2002] and prostate cancer [Wawroschek et al. 1999]. More recently, small handheld detectors have been developed that can provide in situ imaging compatible with surgical and interventional environments. Although these systems cannot provide large field of view images, they may be very useful in tumor resections and image-guided biopsy procedures [Wernick et al. 2004].

## **9.4 Magnetic Resonance Imaging**

### **9.4.1 Basic Physics Concepts**

MRI is based on the phenomenon of nuclear magnetic resonance (NMR). Certain atomic nuclei have inherent magnetic moments, and when these nuclei are placed into a magnetic field, they have a resonant frequency that scales linearly with the magnetic field strength. If these nuclei are subjected to radiofrequency waves at the resonant frequency, they absorb this energy and transition to a higher energy state. These excited nuclei then relax back to their ground state and accordingly emit radiofrequency waves. The relaxation of these nuclei depends strongly on their surroundings, so contrast in the MRI image is based on both the density of nuclei and their chemical environment. For this reason, MRI has much better soft tissue contrast than x-ray-based techniques, since the biochemical properties of soft tissue vary much more than their density or elemental composition. By varying the radiofrequency pulses used to interrogate the tissue, it is also possible to highlight different types of tissue or materials. Thus, contrast mechanisms in the MRI image can be tuned to specific image detection and identification tasks.

### 9.4.2 System Components

An example of MRI scanner is shown in Fig. 9.14. There are three major hardware components to the scanner. The first component is the main magnet that produces the large static magnetic field. This magnetic field is typically 1.5T or greater, which is roughly 30,000 times stronger than the earth's magnetic field. The second component is a series of coils that transmit and receive radio waves from the part of the patient being imaged. The third component is a set of gradient coils, which allows the system to dynamically and spatially vary the magnetic field. Since the resonant frequency of the nuclei is dependent on the magnetic field strength, the gradients allow the system to spatially encode location through frequency and phase variations.



**Fig. 9.14.** Typical MRI scanner. This scanner has a “closed-bore” design, meaning that the patient lies on a bed within a cylindrical bore. The tank on the bed is a test pattern used for calibration of the scanner during maintenance. This particular scanner is used extensively for functional brain imaging, so there are many cables and sensors for providing audiovisual stimulation and feedback to the patient during imaging. Specialty coils for head imaging are seen on the shelf to the left of the scanner

### **9.4.3 Image Characteristics**

It is somewhat difficult to describe a “typical” MRI image, because by varying the parameters of the image acquisition it is possible to create a vast array of possible images from a given region of the body. However, MRI images typically have excellent soft tissue contrast and good spatial resolution, so they are ideal for identifying structures and boundaries.

Image distortion is a potential complicating factor with MRI imaging. Because spatial information is encoded using magnetic field strength, inhomogeneities in the field can cause erroneous shifts in the image data. These inhomogeneities can be caused by the patient, objects worn by the patient, prosthetics/implants, or surgical devices such as frames. Such irregularities in the image pose a particular challenge in image-guided interventions, because they are not easy to characterize in advance (and therefore be corrected).

### **9.4.4 Patient Access and Work Environment**

MRI-based image-guided procedures pose unique challenges. The first challenge is that the high magnetic field creates a very hazardous work environment. The field strength rises rapidly as one approaches the center of the magnet and is strong enough to pull in large, heavy objects such as chairs, gurneys, and oxygen tanks, with potentially fatal results. Small ferromagnetic objects such as scalpels, probes, and paperclips can similarly be turned into dangerous missiles. For this reason, it is critical that every object be evaluated for compatibility before it is brought into the MRI suite. In most cases, this requires investing in a completely separate set of procedural tools and equipment that are dedicated solely to MRI-based interventions.

The second challenge is that the high magnetic fields and radiofrequency radiation can adversely affect electronic devices such as cameras, position trackers, and computers. Some of these devices will completely fail, while others will operate incorrectly or generate artifacts. In most cases, these problems can be mitigated by redesigning the instrument, but again this requires a separate set of devices for the MRI environment.

The third challenge is the amount of available workspace. To create a homogeneous main magnetic field, the bore of the MRI system is long and only slightly wider than the patient, leaving very little room for instruments or even the physician’s hands and arms. Different technical solutions to the limited workspace have been proposed, such as the “double-donut” magnet design, open MRI designs using large flat pole magnets rather than a cylinder, and MRI systems specifically designed with larger bores. However, none of these designs are in widespread use, and the vast majority of MRI systems are not designed with interventions in mind.

### **9.4.5 Current Research and Development Areas**

Despite the many challenges involved with interventional and intraoperative MRI, the superb visualization capabilities and the capacity for functional imaging have led to many innovative solutions for MRI-guided interventions.

#### **9.4.5.1 MRI-Based Neurosurgery**

MRI has proven particularly useful, and therefore achieved the most widespread use in intraoperative brain imaging [Albayrak et al. 2004; Jolesz et al. 2002; Mittal and Black 2006; Yrjana et al. 2007]. Brain MRI provides superior soft tissue detail for visualization of the anatomy. Furthermore, functional brain imaging using MRI can determine which regions of the brain are involved in speech, sensory, and motor tasks. Such information is vital during tumor removal since it enables the surgeon to more accurately avoid those important regions. Similarly, the placement of brain stimulators or other assistive devices can benefit from intraprocedure MRI mapping of critical structures.

Methods for intraoperative brain MRI are often classified into low-field, mid-field, and high-field approaches, depending on the type of MRI system used for imaging.

Low-field imaging systems [Lewin and Metzger 2001] (approximately 0.1T main magnet field strength) tend to have limited imaging capabilities and almost no capacity for functional imaging; however, the low-field strength enables them to be very compact and movable, and requires less modification to the operating room environment. These systems can be thought of as MR-based surgical microscopes, in that they can be added to an existing operating room. Although such systems could, in principle, make intraoperative MRI guidance a more widely available technology, many practitioners feel that the poor image quality severely hampers the clinical utility of these systems.

Mid-field systems [Schwartz et al. 2001] (approximately 0.5T main magnet field strength) are something of a compromise between imaging capability and the restrictions of the operating room, although chronologically these were actually the first systems to be developed. In these systems the main magnet can be more open than that on a conventional scanner, which allows the physician to stand right beside the patient, although the available space is still quite limited. Specialized MRI-compatible equipment and rooms are still required, but a key advantage is that the patient does not have to be moved to acquire images.

High-field systems [Truwit and Hall 2001] (1.5T main magnet field strength and higher) are typically implemented as a multiroom operating suite, where a patient is in one location for the surgery, but can be moved or rotated into an MRI scanner for imaging. The MRI scanner may be behind a

door or other form of shielding, but the operating suite still must maintain a very high level of MRI compatibility. The main advantage of this approach is that it produces very high quality images and functional data, since the scanner is on par with normal diagnostic MRI devices. However, the time required to move the patient between the operating area and the imaging area limits the number of images that can be practically acquired. This type of system is also generally the most expensive and complex to implement because of the large physical space requirements.

#### **9.4.5.2 MRI-Based Interventional Radiology**

Interventional radiology makes use of natural pathways in the body, primarily the circulatory system, to deliver therapy. Catheters and probes are inserted into large vessels and then navigated through the vasculature to the intended target. Although interventional radiology has traditionally been performed with x-ray-based methods such as fluoroscopy, MRI is an attractive image guidance method for several reasons. First, the space requirements for an interventional radiology procedure are relatively low, and it is possible to perform these procedures without having the physician standing directly next to the patient. Thus, the confined quarters of the MRI scanner represent less of a challenge. Second, fluoroscopy exposes both patients and staff to ionizing radiation, which can be especially harmful during long procedures or in sensitive populations such as children. Third, MRI offers potentially significant improvements in visualization over fluoroscopy, including identification of vessels without using contrast and full 3D image acquisition.

Interventional MRI has shown encouraging successes in its early trials, especially in the arena of cardiovascular procedures. In cases of abdominal aortic aneurysm or thoracic aortic dissection, where flow and vessel structure are complex, the visualization benefits of 3D MRI can be advantageous. MRI also can provide improved visualization of the myocardium for many procedures, including delivery of therapeutic materials, placement of prosthetic devices, and electrophysiological corrections [Ozturk et al. 2005].

Naturally, as with MRI-based neurosurgery, there are significant equipment and facilities costs associated with construction of an MRI-based interventional radiology suite, and only a handful of hospitals have access to this level of technology. Furthermore, most commercial MRI scanners are optimized for the diagnostic imaging process (where image quality is paramount) rather than interventional techniques (where some image quality may be sacrificed for real-time performance), so interventional MRI requires a high level of engineering expertise. Finally, the ongoing financial costs of interventional MRI are expected to be higher than that with conventional interventional radiology, because the cost of consumables will likely be larger, although it is too early to tell if the same economies of scale will apply once interventional MRI becomes more prevalent. For these reasons,

MRI-based interventional radiology is still primarily a research area and has not yet achieved widespread clinical use.

### **9.4.5.3 MRI-Based Prostate Therapy and Robotics**

MRI offers several advantages for prostate imaging, including excellent definition of anatomical boundaries, improved visualization of tumor extension and invasion, and the capacity for spectroscopic analysis of tissue. Thus, localized prostate therapies such as brachytherapy could benefit from MRI-based guidance as they would enable improved targeting. However, the standard lithotomy positioning/peritoneal access used for prostate therapies has the patient lying on their back with their legs and feet suspended in stirrups, a position that would be impossible to achieve in a conventional MRI scanner. Thus, investigators have developed specialized MRI scanners to allow prostate brachytherapy to be done inside the imager itself, along with a host of associated technologies for real-time imaging and treatment planning [D'Amico et al. 1998; Haker et al. 2005]. This approach to prostate therapy has demonstrated encouraging clinical results, but has not been adopted at many other sites, in part because of its cost and complexity versus ultrasound, which is used for the majority of prostate brachytherapy implants.

Because the typical MRI scanner is such a cramped work environment, MRI-based interventions benefit from remotely controlled robots that can operate inside the scanner, providing dexterous manipulation in spaces where a person could not work. With robotics, the physician or operator can be outside the scanner or even in another room. Although robots typically have extensive metal and electronic components that would be incompatible with the MRI environment, innovative technologies using pneumatics and plastics have been used to create robots that are compatible with most types of imaging modalities, including MRI [Stoianovici 2005]. These components have been used to develop robotic systems for brachytherapy seed placement or other needle-based therapies in the prostate, and can be deployed in conventional diagnostic MRI scanners [Stoianovici et al. 2007].

## **9.5 Ultrasound**

### **9.5.1 Basic Physics Concepts**

For ultrasound imaging, sound waves in the frequency range of 5–10 MHz are transmitted into the body by a handheld transducer. These waves readily penetrate into soft tissue, but are reflected at tissue boundaries because of the mismatch between the speed of sound in the different tissues. Ultrasound waves used in medicine are stopped by air (because the density of air is too low) and bone (because the density and stiffness of bone is too high). This means that the transducer must be aimed to avoid these structures, and that

overlying bones or air masses will block the imaging of objects deeper in the body. This has several important implications for image-guided interventions. In the thorax, the ultrasound transducer must be placed in the intercostal space between the ribs in order to image organs such as the liver, but the lungs cannot be imaged at all. In the abdomen and pelvis, ultrasound excels because the ribs do not present a barrier, but digestive system gas can potentially be a problem. In the brain, the skull represents a solid bone barrier, effectively precluding ultrasound imaging.<sup>3</sup>

Ultrasound at diagnostic wavelengths and power levels poses no risk to either the operator or the patient, which is one of the reasons why ultrasound is the dominant modality for fetal imaging. This property is also a significant benefit to researchers working in image-guided interventions, since it means that ultrasound systems can be easily used in the lab or office environment.

Because ultrasound works with reflected sound waves, the Doppler effect enables straightforward imaging and quantification of motion within the body. Ultrasound is therefore used extensively in cardiac and vascular imaging, where dynamic features such as flow, turbulence, ventricle wall motion, and valve opening/closing can readily be observed.

### 9.5.2 System Components

Figure 9.15 shows a typical medical ultrasound imaging system. The computer system and display are mounted on a small wheeled cart that allows the system to be easily moved from room to room. Several different probes can be attached to the computer system; each probe has a specific frequency range and shape designed to match a particular imaging task.

The ultrasound transducer can take on many forms. A single element transducer interrogates a line of tissue in front of it, so the simplest possible system would be a single element that was moved over the organ of interest. In practice, however, this method provides too little information to the physician and is also too slow to be clinically useful. The most common system approach is to have either a single element that is mechanically oscillated across the imaging area or a linear array of elements. These are referred to as 2D transducers since their field of view is a single slice. Recently, some system vendors have developed 3D transducers, where a linear array of elements is oscillated across the field, or the transducer has a multi-row array of elements.

---

<sup>3</sup> There is a notable exception to this statement. Because the skull is relatively thin, low-frequency ultrasound waves are able to pass through the skull and image the brain. However, this is a very atypical application for ultrasound, although it is an active and intriguing area of research.



**Fig. 9.15.** Photograph of a medical ultrasound imaging system. As with most ultrasound units, the entire system is on a wheeled cart, so it can easily be moved around the hospital. The integrated system includes a keyboard, additional imaging controls, a monitor for viewing the images, and a small printer for hardcopy output. Different ultrasound probes and other supplies for imaging can also be stored on the cart

Since ultrasound is inherently a real-time modality, some ultrasound scanners offer a 4D imaging mode that allows for visualization of dynamic processes. This scanning mode is essentially 3D imaging at video rates. Because these images contain a large amount of data, they are often presented as a rendered and lighted 3D surface that changes with time. This method is especially useful in cardiac and fetal imaging where there is a clear and easily identifiable structure of interest.

### **9.5.3 Image Characteristics**

Some representative ultrasound images are shown in Fig. 9.16. Several particular characteristics of these images are immediately apparent. The first is that the image is grainy; this appearance is the result of speckle, a non-coherent reflection phenomenon that is endemic to any form of reflection imaging. The second is that the field of view of the image is limited to a 2D wedge-shaped area emerging from end of the probe. The effective viewing depth of a typical medical ultrasound system is about 20 cm, so unlike other



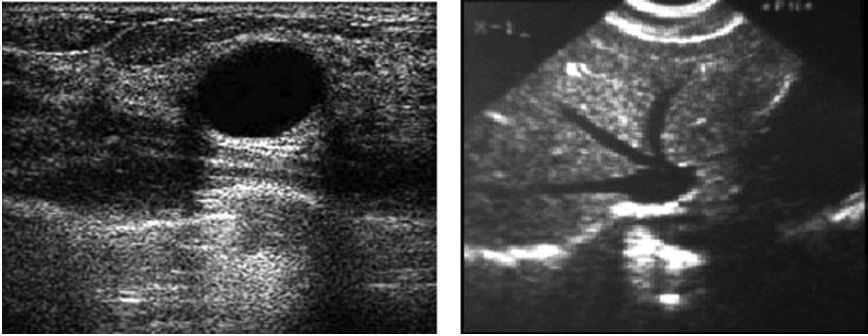


**Fig. 9.16** Ultrasound images of a cyst in the breast (*left image*) and vascular structure in the liver (*right*)

modalities, ultrasound is a regional imaging modality and cannot provide full cross-sectional slices of the body.

### **9.5.4 Patient Access and Work Environment**

Because ultrasound probes are small enough to be handheld, patient access is unsurpassed. Subject to the constraints of overlying bone and air structures, the probe can be easily repositioned to change the field of view or clear the way of a surgical instrument. Probes also can be inserted into body cavities or surgical fields for close access to the object being imaged. Furthermore, even though most ultrasound systems are already on a small, wheeled computer cart, complete imaging systems have been miniaturized to work with portable computers so that the entire system can fit into an even smaller footprint.

The use of a handheld probe poses some interesting problems for ultrasound guidance systems. Because the probe must be pressed tightly against the skin, either the physician or an assistant must be holding the probe at all times, which leaves only one hand for other tasks. A more subtle problem is that the arbitrary orientation of the ultrasound probe can present images that are quite different from conventional cross-sectional imaging (e.g., CT, MRI) to the physician. The physician must therefore mentally integrate the oblique ultrasound view into their reference frame, and this can be a challenging task for new practitioners.

### **9.5.5 Current Research and Development Areas**

#### **9.5.5.1 Ultrasound Registration to Other Modalities**

Because ultrasound provides real-time imaging capabilities in a small form factor without the use of ionizing radiation, there is great interest in combining ultrasound with other imaging modalities. In these approaches, cross-sectional images of the patient and fiducial markers are first obtained using

MRI or CT. The fiducial markers or anatomic landmarks are used to establish a coordinate reference frame for cross-sectional images. A tracked ultrasound probe (typically using optical or electromagnetic tracking; see Chapter 2 for more information) is then registered to the reference frame. As the ultrasound probe is moved around the patient, its position and pose in the tracker frame can be transformed to a position and pose in the reference frame. By resampling and reslicing the cross-sectional image data, a CT or MRI image corresponding to the “live” ultrasound image can be generated and displayed, either as an overlay or a side-by-side image. Image processing techniques, where the view seen by the ultrasound system is dynamically matched to cross-sectional image views obtained in another modality, may also be utilized. This approach has the advantage of not strictly requiring a position tracking system, although it is also more susceptible to variations and artifacts in the images themselves.

Prostate brachytherapy is a good candidate for image fusion; ultrasound is used to guide the implantation of the radioactive seeds, but the ultrasound images may not show as much tissue detail or define the anatomy as well as other modalities. Furthermore, the combination of imaging modalities can provide better postimplant dosimetry by improving visualization of critical structures in combination with the seeds themselves. Ultrasound fusion with both MRI [Daanen et al. 2006; Kaplan et al. 2002; Reynier et al. 2004] and CT/fluoroscopy [French et al. 2005; Fuller et al. 2005; Rubens et al. 2006; Su et al. 2007] has been used in prostate brachytherapy.

Ultrasound registration to CT and MRI is also of great benefit during procedures in the abdomen and thorax. In these regions of the body, involuntary motions such as respiration, peristalsis, and heartbeat can create significant displacements and deformation of organs, and the real-time imaging capabilities of ultrasound provide a great benefit to the physician. By being able to overlay the cross-sectional imaging data on the ultrasound, diagnostic capabilities can be much enhanced [Huang et al. 2005] and intra-procedure navigation can be improved [Beller et al. 2007]. Although motion and deformation of organs is clearly a major challenge in these procedures, as the CT or MRI are most often acquired during a breath hold, the use of landmarks such as vessels [Lange et al. 2003] and mathematical modeling of respiration [Blackall et al. 2005] are being used to address these challenges.

Ultrasound-to-CT registration also has become of great interest in external beam radiation therapy, where it is used to determine the location of the target organ prior to delivery of therapy. Radiation therapy plans are usually derived from a single CT volume acquired before the start of treatment, but anatomical changes in the patient can cause the target organ to shift within the body, so that the pretreatment CT is no longer an accurate image of the patient. The prostate, in particular, can move several millimeters from day to day because of differences in bowel and bladder filling.

To mitigate these anatomical variations, an ultrasound unit referenced to the coordinate frame of the linear accelerator or the treatment room is used to image the patient immediately before the delivery of therapy. The ultrasound is compared to the planning CT and the therapist then moves the patient table to compensate for any changes. This process helps to ensure that the target organ is once again in the proper location for treatment.

### 9.5.5.2 Ultrasound Contrast Agents

Ultrasound contrast agents are similar to those used in x-ray imaging and MRI, in that they provide information about the patient that would not normally be obtainable with that modality. For example, an x-ray contrast agent is a dense material, usually iodine or barium, introduced into a body compartment (such as the vasculature) to change the x-ray attenuation of that structure and increase its conspicuity. Gadolinium and superparamagnetic iron oxide (SPIO) are used as MRI contrast agents because they affect the local magnetic field experienced by the tissue, and therefore the relaxation times of the nuclei. Contrast agents in the blood are often used to identify tumors, since most tumors have an excessively fenestrated capillary bed, which allows the contrast agent to preferentially leak out into the surrounding tissue.

The predominant type of ultrasound contrast agent is the microbubble, a tiny sphere (1–5  $\mu\text{m}$  diameter) that can easily pass through the entire circulatory system. These microbubbles have a polymer shell and an internal core filled with a biologically innocuous gas. The materials and size are chosen so that the microbubbles will strongly reflect the incident ultrasound waves. Because the microbubble is a tuned mechanical system, it also resonates at harmonic frequencies of the input sound wave, enabling the ultrasound system to specifically detect the presence of the contrast agent due to its characteristic resonance.

There are two broad classes of ultrasound contrast agents. The first is the untargeted contrast agent, which travels through the circulatory system much like iodinated CT contrast agents or gadolinium-based MRI agents. Since these agents are designed to remain in the blood pool, they are used primarily in cardiography studies to increase the visibility of the structures in the heart. A handful of these types of agents are FDA approved for regular clinical use. The second class of ultrasound contrast agent is the targeted contrast agent. These agents have a physical structure similar to the untargeted agents, but the shell includes chemicals that allow the microbubble to preferentially bind to biomarkers of disease. Thus, these agents could preferentially define the borders of tumors or allow confirmation of inflammation in important blood vessels. Although initial research in this area has been promising, technology is still developing and none of the targeted ultrasound contrast agents have moved from research into regular clinical use.

### 9.5.5.3 High-Intensity Focused Ultrasound

Although ultrasound in medicine is primarily used for diagnostic imaging, it also can be used therapeutically by increasing the intensity of the transmitted waves. This increased intensity can cause localized heating effects (hyperthermia) or ablate the tissue outright, depending on the energy and the length of time that it is applied. Another important design difference between diagnostic and therapeutic systems is that diagnostic ultrasound typically uses a diverging beam to produce a cone-shaped field of view, whereas therapeutic ultrasound uses a concave transducer or transducer array, which focuses the ultrasound energy onto a point within the body. By moving either the body or the transducer, the focal point can be moved, enabling the treatment of larger body regions.

High-intensity focused ultrasound (HIFU) covers a broad range of transducers and applications. In the prostate, the HIFU transducer is placed in a transrectal probe that also contains an ultrasound imaging system. The ultrasound images provide guidance for positioning of the probe, since prostate anatomy is often imaged using ultrasound. Some studies of the prostate-specific HIFU systems recently have been reported in the literature. According to Murat et al. [2007], results suggest that the technique could be an effective alternative to radiation therapy in certain patient populations.

HIFU is also being used for treatment of breast tumors [Wu et al. 2007], liver and kidney tumors, and uterine fibroids [Leslie and Kennedy 2007]. In these treatments, the ultrasound source is located outside the body and usually integrated with a larger imaging system. Image guidance is provided by either ultrasound imaging or MRI. As these imaging methods are both potentially sensitive to the temperature of the local tissue, imaging can be used to guide and monitor the progress of the therapy, enabling the therapy to be adjusted during treatment to achieve the desired effects.

An important non-oncologic use of HIFU is in the creation of hemostasis following trauma. In many trauma patients, internal bleeding can have severe consequences and is difficult to address without invasive surgery, which naturally carries its own risks and is difficult to perform in the field. HIFU can enable cauterization of vessels and tissue deep inside the body. The principal challenges of this technique are preservation of nearby critical structures and accurate assessment of the bleeding locations, since in most field trauma cases specialized imaging equipment is not readily available [Vaezy et al. 2007].

## 9.6 Summary and Discussion

A summary of the different imaging systems' properties is provided in Table 9.1. There are some notable themes which emerge from this comparison chart:

1. It is clear that no single modality is superior in all areas, and in fact, the modalities are often complementary to each other. For example, some modalities have excellent real-time capability (ultrasound and fluoroscopy), whereas others are more suited to pretreatment imaging, but have better soft tissue visualization, such as MRI and CT. Thus, bridging these gaps (e.g., by combining ultrasound and CT) is a common theme in image-guided interventions research and in image registration in general (this topic is covered more fully in Chapter 6: Rigid Registration and Chapter 7: Nonrigid Registration for Image-Guided Interventions) and is a critical support technology for these efforts.

**Table 9.1.** Summary chart of imaging modalities and their relative strengths and limitations in the context of image-guided interventions

<b>Modality</b>	<b>Strengths</b>	<b>Limitations</b>
Fluoroscopy	<ul style="list-style-type: none"> <li>▪ Sub-millimeter spatial resolution</li> <li>▪ Real-time imaging</li> <li>▪ Good patient access</li> </ul>	<ul style="list-style-type: none"> <li>▪ Limited to 2D projections</li> <li>▪ Requires ionizing radiation</li> <li>▪ Poor soft tissue contrast</li> </ul>
CT	<ul style="list-style-type: none"> <li>▪ Sub-millimeter spatial resolution</li> <li>▪ Fast coverage of large volumes</li> <li>▪ Generates 3D volumes</li> <li>▪ Moderate patient access</li> <li>▪ Provides unique biochemical and functional information</li> </ul>	<ul style="list-style-type: none"> <li>▪ Small number of systems with CT fluoro option</li> <li>▪ Requires ionizing radiation</li> <li>▪ Image formation requires several minutes</li> </ul>
PET/SPET	<ul style="list-style-type: none"> <li>▪ Sensitive to nanomolar amounts of tracer</li> </ul>	<ul style="list-style-type: none"> <li>▪ Requires ionizing radiation</li> <li>▪ Spatial resolution ~ 2–3 mm</li> </ul>
MRI	<ul style="list-style-type: none"> <li>▪ Millimeter spatial resolution</li> <li>▪ Excellent soft tissue contrast</li> <li>▪ Can also image functional information</li> <li>▪ No ionizing radiation</li> <li>▪ Real-time imaging</li> <li>▪ Excellent imaging of flow and motion</li> </ul>	<ul style="list-style-type: none"> <li>▪ Magnetic field creates potential hazards</li> <li>▪ Specialized MRI-compatible equipment needed</li> <li>▪ Limited real-time capabilities</li> <li>▪ Limited, wedge-shaped field of view</li> </ul>
Ultrasound	<ul style="list-style-type: none"> <li>▪ No ionizing radiation</li> <li>▪ Handheld probes with excellent patient access</li> </ul>	<ul style="list-style-type: none"> <li>▪ Images contaminated by speckle</li> <li>▪ Most systems limited to 2D imaging</li> </ul>

2. Many researchers are also attempting to expand the capabilities of a particular modality to make it more compatible with image-guided interventions. For example, more CT scanners are capable of fluoroscopic acquisition, and frame rates are now as high as 8 Hz. Likewise, many ultrasound systems are incorporating array transducers that allow acquisition of a 3D volume image rather than a single 2D slice. With sufficient acquisition speed, the 3D volume can be acquired rapidly, allowing excellent visualization of moving structures such as heart valves.
3. Since image-guided interventions are usually performed using physical tools, such as forceps, the ideal would be for the imaging system to clearly and accurately image those tools as they move inside the patient. Ultrasound and fluoroscopy are, for the most part, capable of this task, but other modalities with poor real-time imaging are not as effective. Therefore, technologies for instrument tracking within the imaging space and inside the patient are an active development area, and registration is essential for ensuring that the image coordinates match those of the tracking system.

## Acknowledgments

The author wishes to thank the faculty and staff of the Department of Radiology at Georgetown University Hospital, the Center for Functional and Molecular Imaging at Georgetown University, and the Department of Radiology at the University of California, San Francisco, for assistance with images gathered for this chapter.

## References

- Albayrak B, Samdani AF, and Black PM. (2004). "Intra-operative magnetic resonance imaging in neurosurgery." *Acta Neurochir (Wien)*, 146(6), 543–556; discussion 557.
- Archer BR. (2006). "Radiation management and credentialing of fluoroscopy users." *Pediatr Radiol*, 36(Suppl 14), 182–184.
- Beller S, Hunerbein M, Lange T, Eulenstein S, Gebauer B, and Schlag PM. (2007). "Image-guided surgery of liver metastases by three-dimensional ultrasound-based optoelectronic navigation." *Br J Surg*, 94(7), 866–875.
- Beyer T, Townsend DW, Brun T, Kinahan PE, Charron M, Roddy R, Jerin J, Young J, Byars L, and Nutt R. (2000). "A combined PET/CT scanner for clinical oncology." *J Nucl Med*, 41(8), 1369–1379.
- Blackall JM, Penney GP, King AP, and Hawkes DJ. (2005). "Alignment of sparse freehand 3-D ultrasound with preoperative images of the liver using models of respiratory motion and deformation." *IEEE Trans Med Imaging*, 24(11), 1405–1416.
- Bushberg J, Seibert J, Leidholdt E, and Boone J. (2002). *The Essential Physics of Medical Imaging, 2nd edition*, Lippincott Williams & Wilkins, Baltimore.

- D'Amico AV, Cormack R, Tempany CM, Kumar S, Topulos G, Kooy HM, and Coleman CN. (1998). "Real-time magnetic resonance image-guided interstitial brachytherapy in the treatment of select patients with clinically localized prostate cancer." *Int J Radiat Oncol Biol Phys*, 42(3), 507–515.
- Daanen V, Gastaldo J, Giraud JY, Fournere P, Descotes JL, Bolla M, Collomb D, and Troccaz J. (2006). "MRI/TRUS data fusion for brachytherapy." *Int J Med Robot*, 2(3), 256–261.
- Endo M, Yoshida K, Kamagata N, Satoh K, Okazaki T, Hattori Y, Kobayashi S, Jimbo M, Kusakabe M, and Tateno Y. (1998). "Development of a 3D CT-scanner using a cone beam and video-fluoroscopic system." *Radiat Med*, 16(1), 7–12.
- French D, Morris J, Keyes M, Goksel O, and Salcudean S. (2005). "Computing intraoperative dosimetry for prostate brachytherapy using TRUS and fluoroscopy." *Acad Radiol*, 12(10), 1262–1272.
- Fuller DB, Jin H, Koziol JA, and Feng AC. (2005). "CT-ultrasound fusion prostate brachytherapy: a dynamic dosimetry feedback and improvement method. A report of 54 consecutive cases." *Brachytherapy*, 4(3), 207–216.
- Gulec SA, Eckert M, and Woltering EA. (2002). "Gamma probe-guided lymph node dissection ('gamma picking') in differentiated thyroid carcinoma." *Clin Nucl Med*, 27(12), 859–861.
- Haker SJ, Mulkern RV, Roebuck JR, Barnes AS, Dimaio S, Hata N, and Tempany CM. (2005). "Magnetic resonance-guided prostate interventions." *Top Magn Reson Imaging*, 16(5), 355–368.
- Hasegawa B, Gingold E, Reilly S, Liew S, and Cann C. (1990). "Description of a simultaneous emission-transmission CT system." *Proc Soc Photo Opt Instrum Eng*, 1231, 50–60.
- Herman GT, and Liu HK. (1977). "Display of three-dimensional information in computed tomography." *J Comput Assist Tomogr*, 1(1), 155–160.
- Huang X, Hill NA, Ren J, Guiraudon G, Boughner D, and Peters TM. (2005). "Dynamic 3D ultrasound and MR image registration of the beating heart." *Med Image Comput Comput Assist Interv Int Conf Med Image Comput Comput Assist Interv*, 8(Pt 2), 171–178.
- Jaffray DA, Siewerdsen JH, Wong JW, and Martinez AA. (2002). "Flat-panel cone-beam computed tomography for image-guided radiation therapy." *Int J Radiat Oncol Biol Phys*, 53(5), 1337–1349.
- Jolesz FA, Talos IF, Schwartz RB, Mamata H, Kacher DF, Hynynen K, McDannold N, Saivironporn P, and Zao L. (2002). "Intraoperative magnetic resonance imaging and magnetic resonance imaging-guided therapy for brain tumors." *Neuroimaging Clin N Am*, 12(4), 665–683.
- Kaplan I, Oldenburg NE, Meskill P, Blake M, Church P, and Holupka EJ. (2002). "Real time MRI-ultrasound image guided stereotactic prostate biopsy." *Magn Reson Imaging*, 20(3), 295–299.
- Lakshminarayanan AV. (1975). *Reconstruction from divergent x-ray data*, State University of New York, Buffalo NY.
- Lange T, Eulenstein S, Hunerbein M, and Schlag PM. (2003). "Vessel-based non-rigid registration of MR/CT and 3D ultrasound for navigation in liver surgery." *Comput Aided Surg*, 8(5), 228–240.

- Leslie TA, and Kennedy JE. (2007). "High intensity focused ultrasound in the treatment of abdominal and gynaecological diseases." *Int J Hyperthermia*, 23(2), 173–182.
- Lewin JS, and Metzger AK. (2001). "Intraoperative MR systems. Low-field approaches." *Neuroimaging Clin N Am*, 11(4), 611–628.
- McRobbie DW, Pritchard S, and Quest RA. (2003). "Studies of the human oropharyngeal airspaces using magnetic resonance imaging. I. Validation of a three-dimensional MRI method for producing *ex vivo* virtual and physical casts of the oropharyngeal airways during inspiration." *J Aerosol Med*, 16(4), 401–415.
- Mittal S, and Black PM. (2006). "Intraoperative magnetic resonance imaging in neurosurgery: the Brigham concept." *Acta Neurochir Suppl*, 98, 77–86.
- Murat FJ, Poissonnier L, Pasticier G, and Gelet A. (2007). "High-intensity focused ultrasound (HIFU) for prostate cancer." *Cancer Control*, 14(3), 244–249.
- Ozturk C, Guttman M, McVeigh ER, and Lederman RJ. (2005). "Magnetic resonance imaging-guided vascular interventions." *Top Magn Reson Imaging*, 16(5), 369–381.
- Reynier C, Troccaz J, Fournier P, Dusserre A, Gay-Jeune C, Descotes JL, Bolla M, and Giraud JY. (2004). "MRI/TRUS data fusion for prostate brachytherapy. Preliminary results." *Med Phys*, 31(6), 1568–1575.
- Rubens DJ, Yu Y, Barnes AS, Strang JG, and Brasacchio R. (2006). "Image-guided brachytherapy for prostate cancer." *Radiol Clin North Am*, 44(5), 735–748, viii–ix.
- Schwartz RB, Kacher DF, Pergolizzi RS, and Jolesz FA. (2001). "Intraoperative MR systems. Midfield approaches." *Neuroimaging Clin N Am*, 11(4), 629–644.
- Scudder H. (1978). "Introduction to computer aided tomography." *Proc IEEE*, 66, 628.
- Stoianovici D. (2005). "Multi-imager compatible actuation principles in surgical robotics." *Int J Med Robot*, 1(2), 86–100.
- Stoianovici D, Song D, Petrisor D, Ursu D, Mazilu D, Mutener M, Schar M, and Patriciu A. (2007). "MRI Stealth" robot for prostate interventions." *Minim Invasive Ther Allied Technol*, 16(4), 241–248.
- Su Y, Davis BJ, Furutani KM, Herman MG, and Robb RA. (2007). "Seed localization and TRUS-fluoroscopy fusion for intraoperative prostate brachytherapy dosimetry." *Comput Aided Surg*, 12(1), 25–34.
- Truwit CL, and Hall WA. (2001). "Intraoperative MR systems. High-field approaches." *Neuroimaging Clin N Am*, 11(4), 645–650, viii.
- Vaezy S, Zderic V, Karmy-Jones R, Jurkovich GJ, Cornejo C, and Martin RW. (2007). "Hemostasis and sealing of air leaks in the lung using high-intensity focused ultrasound." *J Trauma*, 62(6), 1390–1395.
- Valentin J. (2000). "Avoidance of radiation injuries from medical interventional procedures." *Ann ICRP*, 30(2), 7–67.
- Wawroschek F, Vogt H, Weckermann D, Wagner T, and Harzmann R. (1999). "The sentinel lymph node concept in prostate cancer – first results of gamma probe-guided sentinel lymph node identification." *Eur Urol*, 36(6), 595–600.
- Webb A. (2002). *Introduction to Biomedical Imaging, 1st edition*, Wiley-IEEE Press, Hoboken, NJ.



- Wernick M, Brankov J, Chapman D, Anastasio M, Zhong Z, Muehleman C, and Li J. (2004). "Multiple-image Computed Tomography." *IEEE International Symposium on Biomedical Imaging: From Nano to Macro*, Arlington, VA.
- Wu F, ter Haar G, and Chen WR. (2007). "High-intensity focused ultrasound ablation of breast cancer." *Expert Rev Anticancer Ther*, 7(6), 823–831.
- Yrjana SK, Tuominen J, and Koivukangas J. (2007). "Intraoperative magnetic resonance imaging in neurosurgery." *Acta Radiol*, 48(5), 540–549.